nature immunology

NLRP4 negatively regulates type I interferon signaling by targeting the kinase TBK1 for degradation via the ubiquitin ligase DTX4

Jun Cui[1–3,7], Yinyin Li[1,3,4,7], Liang Zhu[1], Dan Liu[5], Zhou Songyang[5], Helen Y Wang[1,3] & Rong-Fu Wang[1,3,6]

Stringent control of the type I interferon signaling pathway is important for maintaining host immune responses and homeostasis, yet the molecular mechanisms responsible for its tight regulation are still poorly understood. Here we report that the pattern-recognition receptor NLRP4 regulated the activation of type I interferon mediated by double-stranded RNA or DNA by targeting the kinase TBK1 for degradation. NLRP4 recruited the E3 ubiquitin ligase DTX4 to TBK1 for Lys48 (K48)-linked polyubiquitination at Lys670, which led to degradation of TBK1. Knockdown of either DTX4 or NLRP4 abrogated K48-linked ubiquitination and degradation of TBK1 and enhanced the phosphorylation of TBK1 and the transcription factor IRF3. Our results identify a previously unrecognized role for NLRP4 in the regulation of type I interferon signaling and provide molecular insight into the mechanisms by which NLRP4-DTX4 targets TBK1 for degradation.

The initiation of innate immune responses depends on the detection of pathogen-associated molecular patterns by several classes of germline-encoded pattern-recognition receptors, including Toll-like receptors (TLRs), RIG-I-like receptors, Nod-like receptors (NLRs) and sensors of DNA[1,2]. After stimulation with a pathogen-associated molecular pattern, these pattern-recognition receptors trigger activation of the transcription factor NF-κB, type I interferons and inflammasome signaling pathways, which leads to the production of proinflammatory cytokines and induction of subsequent adaptive immune responses. Whereas TLR3 recognizes viral double-stranded RNA in endosomes and triggers a signaling pathway mediated by the adaptor TRIF, the RNA helicases RIG-I and Mda5 function as cytoplasmic sensors of RNA and activate the mitochondrial signaling adaptor MAVS (VISA, IPS-1 or Cardif) after ligand recognition[1,2]. Studies have shown that RNA polymerase III can serve as an intracellular sensor of viral DNA by transcribing viral AT-rich double-stranded DNA into double-stranded RNA, which in turn stimulates RIG-I and initiates the MAVS-dependent signaling cascade[3,4]. Furthermore, IFI16 and DDX41 function as cytosolic sensors of DNA and interact with the membrane-associated adaptor STING to activate the type I interferon signaling pathway[5,6]. The key adaptors TRIF, MAVS and STING of both RNA and DNA sensors need the kinase TBK1 to activate the transcription factor IRF3, which leads to the induction of type I interferon signaling.

Although type I interferon is required for viral clearance, aberrant production of type I interferon (including IFN-α and IFN-β) can have a pathological role in autoimmune disorders. Thus, tight regulation of type I interferon signaling is critical for maintaining the homeostasis of both innate and adaptive immunity. NLRs represent a large family of cytosolic pattern-recognition receptors that share a typical nucleotide-binding-and-oligomerization domain (Nod), a leucine-rich repeat (LRR) region and a variable amino-terminal effector domain. Many NLRs have been studied extensively as pattern-recognition receptors that trigger relevant signaling pathways after encountering their pathogen-associated molecular pattern or sensing a danger signal[1,2]. In addition, NLRs can function as negative regulators. NLRX1 has been found to inhibit the type I interferon signaling pathway by binding to MAVS[7,8], whereas NLRC5 has a critical role in the negative regulation of intracellular antiviral responses via interaction with RIG-I and Mda5 (refs. 9,10). Although NLRP4 has been reported to negatively regulate NF-κB signaling and autophagic processes through interactions with the kinase IKK and beclin-1, respectively[11,12], its role in the regulation of type I interferon signaling and antiviral immunity remains unknown. In this study we report that NLRP4 served as a negative regulator of the type I interferon signaling pathway by targeting TBK1. NLRP4 recruited the E3 ubiquitin ligase DTX4 for Lys48 (K48)-linked polyubiquitination and degradation of TBK1. Our findings identify the NLRP4-DTX4 axis as an additional signaling cascade for TBK1 degradation to maintain immune homeostasis during antiviral innate immunity.

[1]The Center for Cell and Gene Therapy, Baylor College of Medicine, Houston, Texas, USA. [2]State Key Laboratory of Pharmaceutical Biotechnology, Department of Biochemistry, Nanjing University, Nanjing, China. [3]Center for Inflammation and Epigenetics, The Methodist Hospital Research Institute, Houston, Texas, USA. [4]Institute of Biosciences and Technology, Texas A&M University Health Science Center, Houston, Texas, USA. [5]Department of Biochemistry and Molecular Biology, Baylor College of Medicine, Houston, Texas, USA. [6]Department of Pathology and Department of Immunology, Baylor College of Medicine, Houston, Texas, USA. [7]These authors contributed equally to this work. Correspondence should be addressed to R.-F.W. (rwang3@tmhs.org).

Received 24 October 2011; accepted 13 January 2012; published online 4 March 2012; doi:10.1038/ni.2239

RESULTS

NLRP4 negatively regulates type I interferon signaling

To identify possible roles for members of the NLR family in antiviral immunity, we transfected HEK293T human embryonic kidney cells (293T cells) with an IFN-β luciferase reporter and the internal control renilla luciferase, as well as expression vectors containing candidate genes encoding NLRs, then treated the cells intracellularly for 24 h with the synthetic RNA duplex poly(I:C) to trigger type I interferon signaling; this identified NLRP4 as an inhibitor of activation of the IFN-β luciferase reporter (**Fig. 1a**). Pancreas, testis, placenta and spleen had high expression of human *NLRP4* mRNA (**Supplementary Fig. 1a**). We readily detected NLRP4 protein in 293T cells, THP-1 human monocytes and BxPC-3 human pancreatic cells (**Supplementary Fig. 1b**). As IFN-β activation requires coordination between the activation of NF-κB and that of IRF3, we used an interferon-stimulated response element (ISRE) luciferase reporter (which requires activation by IRF3 only) to evaluate whether the inhibition of type I interferon by NLRP4 was dependent on its inhibitory effect on NF-κB signaling. Intracellular poly(I:C)-induced activity of the ISRE luciferase reporter was potently inhibited by NLRP4 (**Fig. 1a**), which suggested that NLRP4 directly inhibits IFN-β activation by blocking IRF3 signaling. We obtained similar results with 293T-TLR3 cells (293T cells that express TLR3) treated with poly(I:C) (**Fig. 1b**) or 293T cells treated with poly(dA:dT) (**Fig. 1c**) or infected with vesicular stomatitis virus tagged with enhanced green fluorescent protein (VSV-eGFP; **Fig. 1d**), when we transfected the cells with increasing amounts of expression vector for NLRP4. These results suggested that NLRP4 is a negative regulator of the type I interferon signaling pathway.

To determine how NLRP4 inhibits the type I interferon signaling, we assessed the phosphorylation of IRF3 in 293T cells expressing NLRP4 together with RIG-I, Mda5, MAVS or TRIF and found that NLRP4 potently inhibited the phosphorylation of endogenous IRF3 induced by these innate immune receptors and adaptors (**Fig. 1e**). As activation of IFN-β is also associated with the translocation of IRF3 from the cytoplasm into the nucleus, we examined the translocation of endogenous IRF3 in cells with or without expression of GFP-tagged NLRP4. In cells transfected with empty vector, IRF3 rapidly translocated from the cytoplasm to the nucleus after intracellular treatment with poly(I:C). In contrast, IRF3 was retained in the cytoplasm of cells expressing GFP-tagged NLRP4 after stimulation (**Fig. 1f**). These results suggested that NLRP4 inhibits the activation of type I interferon induced by stimulation with double-stranded RNA and DNA or viral infection by blocking the phosphorylation and translocation of IRF3.

Knockdown of *NLRP4* enhances IFN-β and antiviral responses

We next determined whether specific knockdown of endogenous NLRP4 would increase IFN-β expression under physiological conditions. We used an *NLRP4*-specific small interfering RNA (siRNA) and two *NLRP4*-specific lentivirus short hairpin RNA (shRNA) constructs to knock down the expression of NLRP4. All three efficiently inhibited the expression of transfected and endogenous NLRP4 in 293T cells and THP-1 cells (**Fig. 2a** and **Supplementary Fig. 2a–c**). We next assessed the effects of *NLRP4* knockdown on the activation of type I interferon. With the ISRE luciferase reporter assay, we found that knockdown of *NLRP4* resulted in much more activity of the ISRE luciferase reporter triggered by poly(I:C), intracellular poly(I:C), poly(dA:dT) or VSV-eGFP in 293T cells or 293T-TLR3 cells (**Fig. 2b**). To further demonstrate the effects of *NLRP4* knockdown on the expression of interferon-responsive genes, we knocked down *NLRP4* in THP-1 cells and then infected the cells with VSV-eGFP; we found that infection with VSV-eGFP resulted in much higher expression of *IFNB* mRNA and IFN-β protein in cells transfected with *NLRP4*-specific siRNA than in those transfected with siRNA with a scrambled sequence (**Fig. 2c**). Consistent with that, knockdown of *NLRP4* also resulted in higher expression of several interferon-stimulated genes, including *ISG15*, *IFIT2* (which encodes ISG-56), *IFIT1* (which encodes ISG-54) and *CCL5*, after infection with VSV-eGFP (**Fig. 2d**). We obtained similar results with human peripheral blood mononuclear cells (PBMCs) transfected with *NLRP4*-specific siRNA or scrambled siRNA (**Fig. 2e**). These results suggested that knockdown of *NLRP4* enhanced IFN-β activation and the expression of interferon-stimulated genes.

To demonstrate a link between the enhanced type I interferon response and antiviral immunity in cells in which *NLRP4* was knocked down, we knocked down *NLRP4* expression in THP-1 cells and then infected the cells with VSV-eGFP at a multiplicity of infection (MOI) of 1 or 10. Knockdown of *NLRP4* rendered the cells resistant to viral infection and resulted in considerably fewer GFP$^+$ (virus-infected) cells than among cells treated with scrambled siRNA (**Fig. 2f**). Flow cytometry

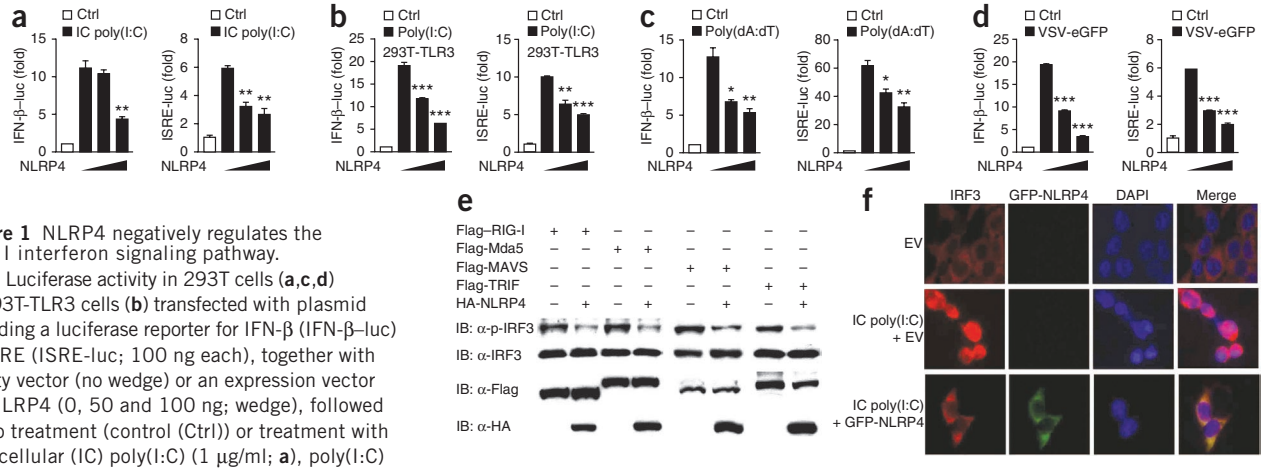

Figure 1 NLRP4 negatively regulates the type I interferon signaling pathway. (**a**–**d**) Luciferase activity in 293T cells (**a**,**c**,**d**) or 293T-TLR3 cells (**b**) transfected with plasmid encoding a luciferase reporter for IFN-β (IFN-β–luc) or ISRE (ISRE-luc; 100 ng each), together with empty vector (no wedge) or an expression vector for NLRP4 (0, 50 and 100 ng; wedge), followed by no treatment (control (Ctrl)) or treatment with intracellular (IC) poly(I:C) (1 μg/ml; **a**), poly(I:C) (10 μg/ml; **b**), poly(dA:dT) (1 μg/ml; **c**) or VSV-eGFP (MOI, 0.01; **d**); results are presented relative to renilla luciferase activity. (**e**) Immunoblot analysis (IB) of total and phosphorylated (p-) IRF3 in 293T cells transfected with various combinations (above lanes) of plasmid for Flag-tagged RIG-I, Mda5, MAVS or TRIF plus vector for HA-tagged NLRP4, probed with antibodies (α-) along left margin. (**f**) Fluorescence microscopy of IRF3 in 293T cells transfected with empty vector (EV) or vector for GFP-tagged NLRP4, then left untreated (top row) or treated with intracellular poly(I:C). DAPI, DNA-intercalating dye. Original magnification, ×40. $^*P < 0.05$, $^{**}P < 0.01$ and $^{***}P < 0.001$, versus cells with the same treatment without NLRP4 expression (two-tailed Student's *t*-test). Data are representative of three independent experiments (mean and s.d. in **a**–**d**).

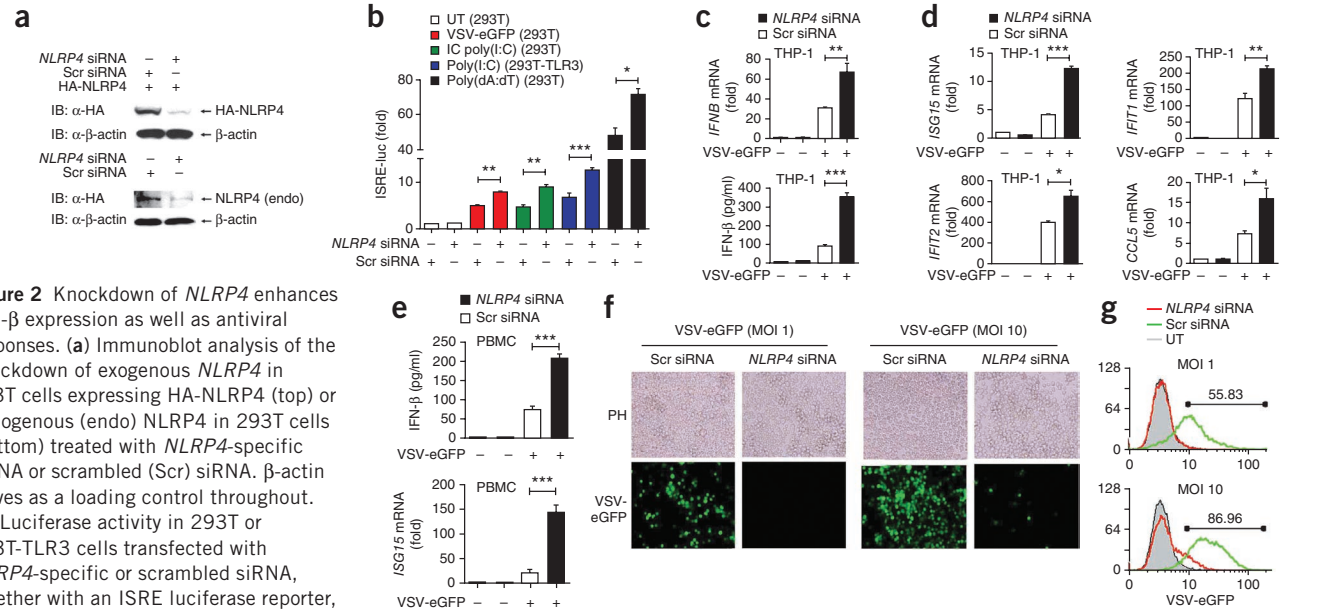

Figure 2 Knockdown of *NLRP4* enhances IFN-β expression as well as antiviral responses. (**a**) Immunoblot analysis of the knockdown of exogenous *NLRP4* in 293T cells expressing HA-NLRP4 (top) or endogenous (endo) NLRP4 in 293T cells (bottom) treated with *NLRP4*-specific siRNA or scrambled (Scr) siRNA. β-actin serves as a loading control throughout. (**b**) Luciferase activity in 293T or 293T-TLR3 cells transfected with *NLRP4*-specific or scrambled siRNA, together with an ISRE luciferase reporter, then left untreated (UT) or treated with VSV-eGFP, intracellular poly(I:C), poly(I:C) or poly(dA:dT) (results presented as in **Fig. 1a–d**). (**c**,**d**) Real-time PCR analysis of *IFNB* mRNA and enzyme-linked immunosorbent assay of IFN-β protein (**c**) and real-time PCR analysis of *ISG15*, *IFIT1*, *IFIT2* and *CCL5* mRNA (**d**) in THP-1 cells treated with *NLRP4*-specific or scrambled siRNA, followed by no infection (–) or infection (+) with VSV-eGFP (MOI, 1); results for mRNA are relative to those of untreated cells. (**e**) Enzyme-linked immunosorbent assay of IFN-β protein and real-time PCR analysis of *ISG15* mRNA in PBMCs treated as in **c**,**d** (mRNA results presented as in **c**,**d**). (**f**,**g**) Phase-contrast (PH) and fluorescence microscopy (**f**) and flow cytometry (**g**) assessing the infection of THP-1 cells left untreated or treated with *NLRP4*-specific or scrambled siRNA, and then infected with VSV-eGFP at an MOI of 1 or 10. Original magnification (**f**), ×10. Numbers above bracketed lines (**g**) indicate percent cells expressing eGFP (infected cells). $^*P < 0.05$, $^{**}P < 0.01$ and $^{***}P < 0.001$, versus cells transfected with scrambled siRNA (two-tailed Student's *t*-test). Data are representative of three independent experiments (mean and s.d. in **b**–**e**).

showed that a low frequency of cells were infected (GFP^+) among THP-1 cells transfected with *NLRP4*-specific siRNA (1% at an MOI of 1, or 11% at an MOI of 10) relative to a greater frequency of GFP^+ cells among cells transfected with scrambled siRNA (55.83% at an MOI of 1, or 87% at an MOI of 10; **Fig. 2g**). These results suggested that *NLRP4*-specific knockdown was able to markedly enhance the type I interferon response and antiviral immunity.

NLRP4 inhibits IRF3 phosphorylation by targeting TBK1

As NLRP4 inhibited activation of the IFN-β luciferase reporter triggered by various stimuli, we next sought to determine the molecular mechanisms by which NLRP4 inhibits type I interferon signaling. We cotransfected 293T cells with expression vector containing *TICAM1* (which encodes TRIF), *DDX58* (which encodes RIG-I), *IFIH1* (which encodes Mda5), *MAVS*, *TMEM173* (which encodes STING), *TBK1* or *IKBKE* (which encodes the kinase IKKi) together with increasing amounts of expression vector containing *NLRP4* plus the IFN-β or ISRE luciferase reporter and found that NLRP4 inhibited activation of the luciferase reporters induced by TRIF, RIG-I, Mda5, MAVS, STING and TBK1 but showed weak or no inhibition of activity of either luciferase reporter induced by IKKi (**Fig. 3a**,**b** and **Supplementary Fig. 3**), which suggested that NLRP4 may inhibit type I interferon signaling by interacting with TBK1. To substantiate the inhibitory function of human NLRP4 in type I interferon signaling, we first assessed the expression of seven mouse homologs (NLRP4a–NLRP4g) of human NLRP4 and found that mouse embryonic fibroblasts and RAW264.7 mouse macrophages had high expression of NLRP4b, NLRP4c, NLRP4e and NLRP4g (**Supplementary Fig. 4a**). We then assessed the biological function of two mouse homologs and found that, like human NLRP4, mouse NLRP4b and NLRP4g strongly inhibited activation of the ISRE luciferase reporter by TBK1 (**Supplementary Fig. 4b**), which suggested that the biological function of NLRP4 may be conserved in humans and mice.

Further coimmunoprecipitation and immunoblot analyses showed that NLRP4 interacted with TBK1 but not with IKKi, IRF3 or IRF7 (**Fig. 3c**). To determine the physiological relevance of those findings, we infected 293T cells with VSV-eGFP and collected cell lysates at various time points. We used antibody to NLRP4 (anti-NLRP4) and anti-IRF3 to immunoprecipitate NLRP4-associated proteins and IRF3-associated proteins, respectively. NLRP4 had little or no interaction with TBK1 in unstimulated 293T cells, but the interaction between NLRP4 and TBK1 increased considerably at 8 h and 10 h after VSV infection. In contrast, we detected neither IKKi nor IRF3 in samples immunoprecipitated with anti-NLRP4 (**Fig. 3d**), which indicated that NLRP4 interacted with TBK1 but not with IKKi or IRF3 under physiological conditions, even after viral infection. As expected, we did not detect TBK1 among proteins immunoprecipitated with anti-IRF3 before viral infection, but we did detect that interaction after infection and found that it peaked at 2–4 h after infection. We also did not observe any interaction between NLRP4 and IRF3 in samples immunoprecipitated with anti-IRF3 (**Fig. 3d**). We obtained similar results with VSV-eGFP–infected THP-1 cells (**Fig. 3e**). To further assess whether NLRP4 interacts with TBK1 in primary cells, we isolated PBMCs and then infected them with VSV-eGFP. We found that the NLRP4-TBK1 interaction was much greater after infection with VSV-eGFP (**Fig. 3f**). These results suggested that NLRP4 interacted with the activated form of TBK1 but not with IKKi or IRF3 after viral infection. To address that possibility, we generated four deletion mutants of TBK1 containing various combinations of the TBK1 domains (**Fig. 3g**). Among all those, the TBK1 mutant containing only the kinase domain interacted with NLRP4, whereas TBK1 mutants containing only the coiled-coil domain or the ubiquitin-like domain plus the coiled-coil

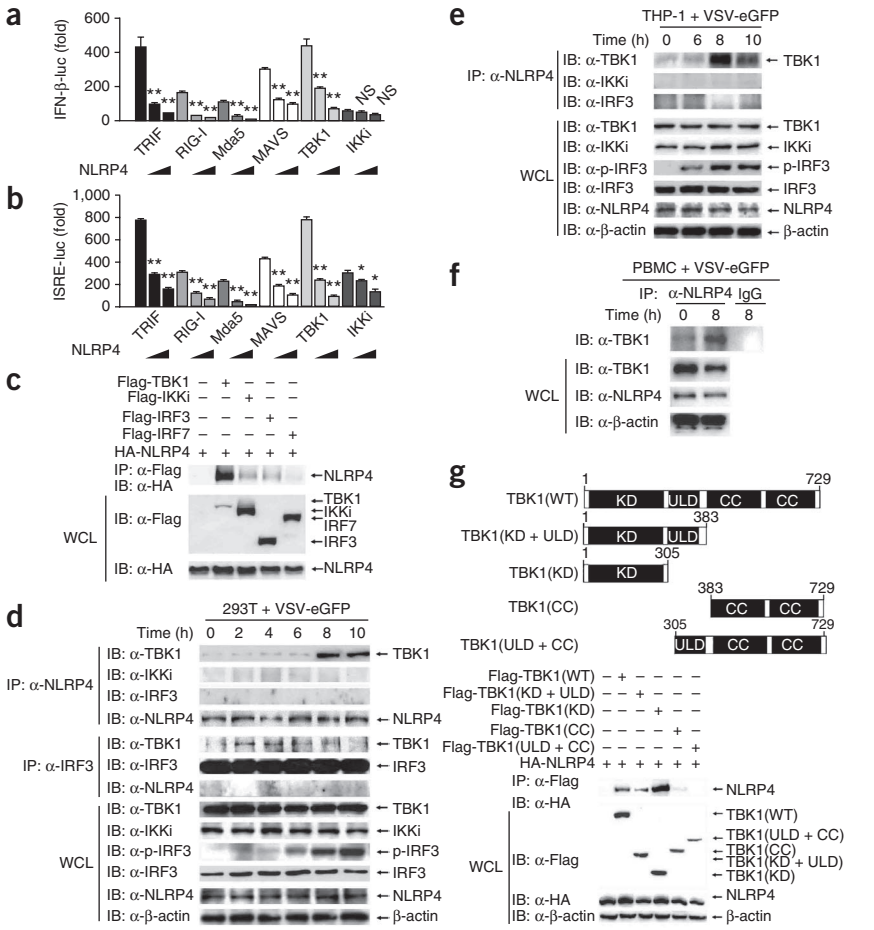

Figure 3 NLRP4 associates with TBK1 to inhibit IRF3 activation. (**a**,**b**) Luciferase activity of 293T cells transfected with an IFN-β (**a**) or ISRE (**b**) luciferase reporter, together with vector for TRIF, RIG-I, Mda5, MAVS, TBK1 or IKKi, along with empty vector (no wedge) or with increasing amounts (wedge) of expression vector for NLRP4 (results presented as in **Fig. 1a**–**d**). (**c**) Immunoassay of 293T cells transfected with vector for HA-NLRP4 together with plasmid for Flag-tagged TBK1, IKKi, IRF3 or IRF7, followed by immunoprecipitation (IP) with anti-Flag beads and immunoblot analysis with anti-HA. WCL, immunoblot analysis of whole-cell lysates without immunoprecipitation (throughout). (**d**) Immunoassay of extracts of 293T cells infected for various times (above lanes) with VSV-eGFP, followed by immunoprecipitation with anti-NLRP4 or anti-IRF3 and immunoblot analysis (antibodies, left margin). (**e**,**f**) Immunoassay of extracts of THP-1 cells (**e**) or PBMCs (**f**) infected for various times (above lanes) with VSV-eGFP, followed by immunoprecipitation with anti-NLRP4 and immunoblot analysis (antibodies, left margin). (**g**) Coimmunoprecipitation and immunoblot analysis (bottom) of 293T cells transfected with deletion mutants of TBK1 (top) along with vector for HA-NLRP4. WT, wild-type; KD, kinase domain; ULD, ubiquitin-like domain; CC, coiled-coil domain. Numbers above indicate amino acid positions. NS, not significant. $^{*}P < 0.01$ and $^{**}P < 0.001$, versus overexpression of RIG-I, Mda5, MAVS, TBK1 or IKKi alone (two-tailed Student's *t*-test). Data are representative of at least three independent experiments (mean and s.d. in **a**,**b**).

domain showed no interaction with NLRP4 (**Fig. 3g**), which indicated that NLRP4 binds to the kinase domain of TBK1.

NLRP4 targets TBK1 for degradation

We next sought to determine how NLRP4 inhibits IRF3 activation through its interaction with TBK1. When we transfected 293T cells with plasmid encoding Flag-tagged TBK1 and hemagglutinin (HA)-tagged IRF3 together with increasing amounts of plasmid encoding NLRP4, we found that the concentration of TBK1 protein diminished considerably with increasing NLRP4 expression (**Fig. 4a**). Consistent with the decrease in TBK1 protein, phosphorylation of IRF3 also decreased with increasing amounts of NLRP4. In contrast, total IRF3 protein was not altered with increasing NLRP4 expression (**Fig. 4a**). Similarly, we also observed much less TBK1 protein in the presence of mouse NLRP4b and NLRP4g (**Supplementary Fig. 4c**). To exclude the possibility that the decrease in TBK1 protein was caused by lower expression of the gene (*TBK1*), we used RT-PCR to analyze the same 293T cells expressing various genes and found that the abundance of *TBK1* mRNA did not change with increasing expression of NLRP4 (**Fig. 4a**). Loss of TBK1 protein induced by NLRP4 was blocked by the proteasome inhibitor MG-132 (**Fig. 4b**), which indicated that NLRP4 caused TBK1 degradation via a proteasome pathway. To determine the specificity of the NLRP4-mediated degradation of TBK1, we did similar experiments with cells expressing IKKα, IKKβ or IKKi with increasing NLRP4 expression and found that NLRP4 specifically induced the degradation of TBK1 but did not affect the concentration of IKKα, IKKβ or IKKi (**Supplementary Fig. 5**). In addition, knockdown of *NLRP4* not only resulted in much more Flag-tagged TBK1 but also enhanced the TBK1-induced activity of the ISRE luciferase reporter relative to that in cells transfected with the control shRNA (**Fig. 4c**,**d**).

In assessing whether NLRP4 is able to mediate degradation of endogenous TBK1 under physiological conditions, we unexpectedly found that endogenous TBK1 was not changed in 293T cells transfected to express NLRP4 alone (**Supplementary Fig. 6a**). As endogenous NLRP4 interacted with TBK1 after infection with VSV, we hypothesized that NLRP4 induces degradation of TBK1 only when type I interferon signaling, in particular TBK1 itself, is activated. To test that possibility, we transfected 293T cells with plasmid encoding HA-NLRP4 or empty vector and infected them with VSV-eGFP. We found much less TBK1 protein in HA-NLRP4–expressing cells infected with VSV-eGFP than in HA-NLRP4–expressing cells without VSV-eGFP infection or in cells transfected with empty vector and infected with VSV-eGFP (**Fig. 4e**). Similarly, after VSV infection, 293T cells transfected to express GFP-tagged NLRP4 had less endogenous TBK1 and phosphorylated IRF3 than did 293T cells transfected with empty vector, whereas the abundance of endogenous IKKi remained the same in both groups of cells (**Supplementary Fig. 6b**). Conversely, knockdown of *NLRP4* resulted in much more endogenous TBK1 in cells infected with VSV-eGFP but not in uninfected cells (**Fig. 4f**). These results suggested that overexpression or knockdown of *NLRP4* was able to change the abundance of TBK1 only in cells infected with virus. As NLRP4 bound to the kinase domain of TBK1 (**Fig. 3g**), we further determined whether NLRP4 bound to phosphorylated (activated) TBK1 to mediate its degradation. We generated a mutant of TBK1 with substitution of alanine for the serine at position 172 (Ser172) in the kinase domain of TBK1 (S172A) and found that NLRP4 did not bind the mutant TBK1 (**Fig. 4g**) or mediate its

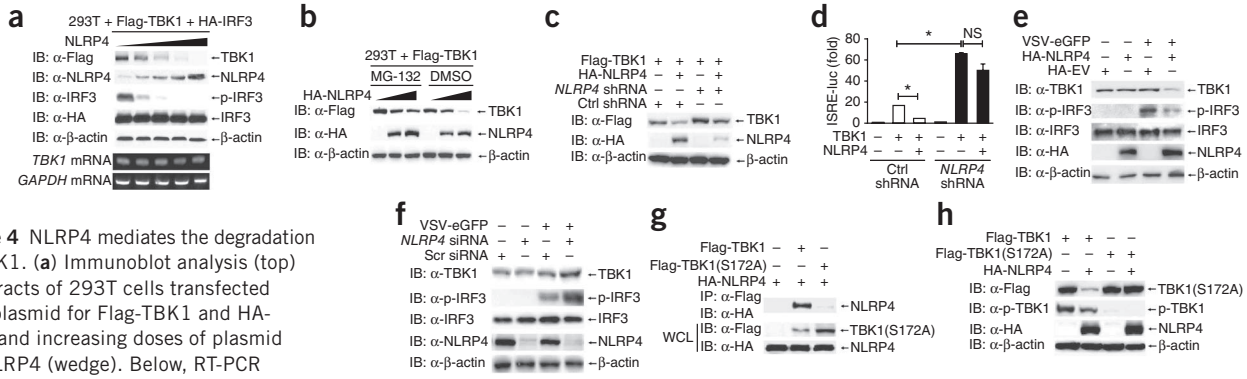

Figure 4 NLRP4 mediates the degradation of TBK1. (**a**) Immunoblot analysis (top) of extracts of 293T cells transfected with plasmid for Flag-TBK1 and HA-IRF3 and increasing doses of plasmid for NLRP4 (wedge). Below, RT-PCR analysis of *TBK1* mRNA; *GAPDH* mRNA (encoding glyceraldehyde phosphate dehydrogenase) serves as a loading control. (**b**) Immunoblot analysis of extracts of 293T cells transfected with plasmid for Flag-TBK1 and HA-NLRP4 (100 or 200 ng; wedges) and treated with dimethyl sulfoxide (DMSO; vehicle) or MG-132. (**c**,**d**) Immunoblot analysis (**c**) and luciferase activity (**d**) of 293T cells transfected with plasmids for Flag-TBK1 and HA-NLRP4, as well as *NLRP4*-specific or control shRNA (**c**,**d**), together with an ISRE luciferase reporter (**d**; results presented as in **Fig. 1a**–**d**). $*P < 0.001$, versus treatment with control shRNA or overexpression of NLRP4 (two-tailed Student's *t*-test). (**e**) Immunoblot analysis of extracts of 293T cells transfected with HA-tagged empty vector (HA-EV) or vector for HA-NLRP4, followed by no infection or infection with VSV-eGFP. (**f**) Immunoblot analysis of extracts of THP-1 cells transfected with *NLRP4*-specific or scrambled siRNA, followed by no infection or infection with VSV-eGFP. (**g**,**h**) Immunoblot analysis of NLRP4 (**g**) and total TBK1(S172A) and phosphorylated TBK1 (**h**) in 293T cells transfected with various combinations (above lanes) of expression vector for NLRP4 and plasmid for Flag-tagged TBK1 or TBK1(S172A), followed by immunoprecipitation with anti-Flag beads. Data are representative of at least three independent experiments (mean and s.d. in **d**).

degradation, in contrast to its binding to the wild-type TBK1 construct (**Fig. 4h**). These results suggested that the phosphorylation of TBK1 at Ser172 was critically required for its interaction with NLRP4.

NLRP4 induces TBK1 ubiquitination after viral infection

To identify the molecular mechanisms by which NLRP4 targets TBK1 for degradation by viral infection, we used a cycloheximide-chase assay determined by the time course of TBK1 degradation after viral infection. We added cycloheximide to 293T cells and THP-1 cells 2 h after VSV-eGFP infection to block protein synthesis. We found that viral infection accelerated TBK1 degradation in both cell types (**Fig. 5a**,**b**). Published studies have shown that viral infection induces K63-linked ubiquitination of TBK1, which is important for activation of the IRF3 signaling pathway[13,14]. In 293T cells that stably expressed HA-tagged K63- or K48-linked ubiquitin, we found that TBK1 was ubiquitinated with K48 and K63 linkage after infection with VSV-eGFP (**Fig. 5c**). In assessing whether NLRP4 was required for TBK1 ubiquitination, we found more K48-linked ubiquitination of TBK1 in cells with coexpression of NLRP4 and TBK1, whereas the amount of K63-linked ubiquitination of TBK1 remained unchanged, relative to that in cells transfected to express TBK1 alone (**Fig. 5d**). Consistent with that observation, knockdown of *NLRP4* resulted in much less K48-linked ubiquitination of TBK1. The K63-linked polyubiquitination of TBK1 was not affected by *NLRP4* knockdown (**Fig. 5e**). These results suggested that NLRP4 specifically induced K48-linked polyubiquitination of TBK1, thus facilitating its degradation after viral infection.

NLRP4 Nod is responsible for TBK1 degradation

To identify which domain of NLRP4 is responsible for TBK1 ubiquitination and degradation, we generated three deletion mutants of NLRP4 containing only the pyrin domain (PYD), Nod or LRR domain and assessed their ability to inhibit TBK1-induced signaling pathways (**Fig. 6a**). We found that full-length NLRP4 and NLRP4 containing only Nod inhibited the TBK1-induced activity of the IFN-β or ISRE luciferase reporter, but NLRP4 containing only PYD or the LRR domain did not (**Fig. 6b**), which suggested that Nod of NLRP4 was responsible for the observed inhibition of TBK1 activity by NLRP4. We further found that like full-length NLRP4, NLRP4 containing only Nod interacted with and caused degradation of TBK1, but NLRP4 containing only PYD or the LRR domain did not (**Fig. 6c**). In addition, NLRP4 containing only Nod interacted with the kinase domain of TBK1 and enhanced the K48-linked ubiquitination of TBK1 but not the K63-linked ubiquitination of TBK1 (**Fig. 6d**,**e**), which suggested that Nod of NLRP4 is required for the ubiquitination and degradation of TBK1. Notably, we observed that NLRP4 induced the degradation of full-length TBK1 but not of any of the truncated TBK1 proteins (**Supplementary Fig. 7**), which suggested that the kinase domain of TBK1 was required for its binding to NLRP4 but was not sufficient for its ubiquitination or degradation.

DTX4 is an E3 ubiquitin ligase for TBK1 ubiquitination

As NLRP4 is not an E3 ubiquitin ligase, we reasoned that NLRP4 might function as an adaptor to recruit an E3 ubiquitin ligase to TBK1. To identify the E3 ubiquitin ligase(s) responsible for TBK1 ubiquitination, we designed an assay to screen for the activity of the ISRE luciferase reporter in 293T cells transfected to express TBK1 and the ISRE luciferase reporter, plus shRNA constructs from a sub-library of shRNAs for human E3 ubiquitin ligases containing a RING domain (a ligase domain that promotes ubiquitination). In an initial screening of about 900 shRNAs, we identified shRNA that targeted the E3 ubiquitin ligase DTX4 and resulted in much more activity of the ISRE luciferase reporter than did control shRNA (**Supplementary Fig. 8a**). To demonstrate the involvement of DTX4 in type I interferon signaling, we first confirmed the knockdown efficiency of *DTX4* by shRNA with real-time PCR and immunoblot analysis (**Supplementary Fig. 8b**–**d**) and then assessed whether specific knockdown of *DTX4* restored the TBK1-induced activity of the ISRE luciferase reporter inhibited by NLRP4. Knockdown of endogenous *DTX4* by various *DTX4*-specific shRNAs markedly abrogated the inhibition of TBK1-induced ISRE activation by NLRP4 (**Fig. 7a**). Consistent with that observation, restoration of the NLRP4-mediated inhibition of TBK1-induced activity of the ISRE luciferase reporter by *DTX4*-specific shRNA correlated well with the ability of *DTX4*-specific shRNA to restore the abundance of TBK1 protein, and the degradation of TBK1 induced by NLRP4 was completely or partially blocked when *DTX4* was knocked down (**Fig. 7a** and **Supplementary Fig. 8e**). We also

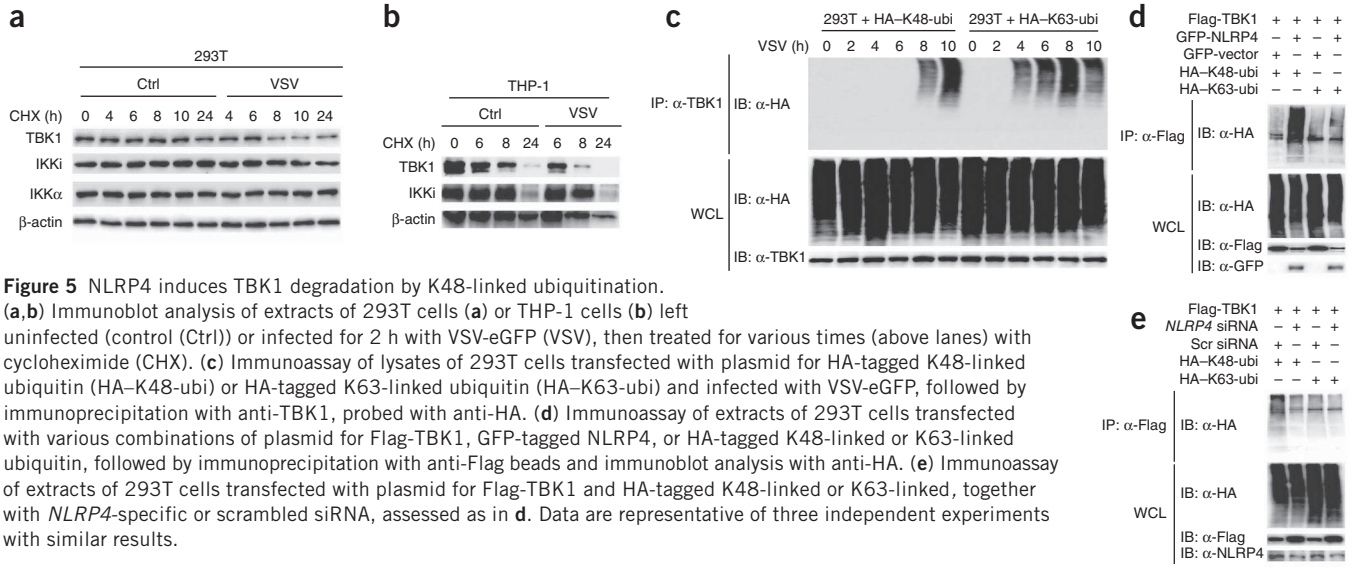

Figure 5 NLRP4 induces TBK1 degradation by K48-linked ubiquitination. (**a**,**b**) Immunoblot analysis of extracts of 293T cells (**a**) or THP-1 cells (**b**) left uninfected (control (Ctrl)) or infected for 2 h with VSV-eGFP (VSV), then treated for various times (above lanes) with cycloheximide (CHX). (**c**) Immunoassay of lysates of 293T cells transfected with plasmid for HA-tagged K48-linked ubiquitin (HA–K48-ubi) or HA-tagged K63-linked ubiquitin (HA–K63-ubi) and infected with VSV-eGFP, followed by immunoprecipitation with anti-TBK1, probed with anti-HA. (**d**) Immunoassay of extracts of 293T cells transfected with various combinations of plasmid for Flag-TBK1, GFP-tagged NLRP4, or HA-tagged K48-linked or K63-linked ubiquitin, followed by immunoprecipitation with anti-Flag beads and immunoblot analysis with anti-HA. (**e**) Immunoassay of extracts of 293T cells transfected with plasmid for Flag-TBK1 and HA-tagged K48-linked or K63-linked, together with *NLRP4*-specific or scrambled siRNA, assessed as in **d**. Data are representative of three independent experiments with similar results.

found that DTX4 expression alone did not cause TBK1 degradation, but coexpression of DTX4 and NLRP4 resulted in more TBK1 degradation than did expression of NLRP4 alone (**Fig. 7b**). Furthermore, we found that NLRP4 and its Nod interacted with DTX4 (**Supplementary Fig. 9a**), whereas the RING domain of DTX4 was critically required for inhibition of activity of the ISRE luciferase reporter as well as interaction with the NLRP4 Nod (**Supplementary Fig. 9b–e**). These results suggested that DTX4 has a critical role in the ubiquitination of TBK1 for proteasome-mediated degradation in an NLRP4-dependent manner.

To determine the sequence of events in the interaction among NLRP4, TBK1 and DTX4 under physiological conditions, we infected Flag-DTX4–expressing cells with VSV-eGFP, then collected cells at various time points after infection and immunoprecipitated complexes from lysates with anti-Flag (for DTX4), anti-TBK1 or anti-NLRP4. Immunoblot analysis showed that DTX4, TBK1 and NLRP4 did not interact in resting cells. We detected interaction between NLRP4 and DTX4 at 6 h; this increased by 8 h after infection. At 8 h after infection, we were able to detect interaction of TBK1 with NLRP4 and DTX4 (**Fig. 7c**). The interaction between DTX4 and TBK1 induced by viral infection was much lower when *NLRP4* was knocked down by *NLRP4*-specific shRNA (**Fig. 7d**). These results suggested that NLRP4 recruits DTX4 to interact with activated TBK1 after viral infection.

Consistent with those observations, we found that ectopic expression of DTX4 and NLRP4 enhanced K48-linked ubiquitination of TBK1 but not K63-linked ubiquitination of TBK1 relative to ubiquitination in the presence of NLRP4 expression alone (**Supplementary Fig. 10a**,**b**). Similarly, knockdown of endogenous *DTX4* resulted in less K48-linked ubiquitination of TBK1 but had no effect on K63-linked polyubiquitination (**Supplementary Fig. 10c**,**d**). To determine the role of endogenous NLRP4 and DTX4 in the ubiquitination of TBK1 during viral infection, we knocked down endogenous *DTX4* or *NLRP4* and assessed TBK1 ubiquitination at 8 and 10 h after viral infection. In cells transfected with control siRNA, we observed considerable K48-linked polyubiquitination of TBK1 (but not K63-linked TBK1 polyubiquitination) at 8 and 10 h after viral infection; however, such polyubiquitination of TBK1 was completely abolished in cells transfected with *NLRP4*- or *DTX4*-specific siRNA (**Fig. 7e**). Furthermore, cells transfected with *NLRP4*- or *DTX4*-specific siRNA had more phosphorylated TBK1 and IRF3 (**Fig. 7e**). Together these data suggested that both NLRP4 and DTX4 were required for the control of TBK1 ubiquitination and degradation and thus the inhibition of IFN-β signaling.

NLRP4 inhibits TBK1-dependent type I interferon signaling

Although most cell types use TBK1-IRF3–dependent type I interferon signaling pathways (for IFN-β production) after viral infection, plasmacytoid dendritic cells use mainly MyD88-IRF7–dependent (TBK1-independent) type I interferon signaling pathways (for IFN-α production) after stimulation with the dinucleotide CpG and viral infection[15]. Spatiotemporal regulation of MyD88–IRF7 signaling by liposomes containing CpG-A and DOTAP (*N*-[1-(2,3-dioleoyloxy)propyl]-*N*,*N*,*N*-trimethylammonium methyl-sulfate) leads to robust production of IFN-α in macrophages, whereas treatment with CpG-A does not[16]. In determining whether NLRP4-DTX4 inhibited TBK1-dependent, but not MyD88-IRF7–dependent, type I interferon signaling, we first found no interaction between NLRP4 and MyD88 (**Supplementary Fig. 11**). We next transfected PBMCs and THP-1 cells with scrambled siRNA, *NLRP4*-specific siRNA or *DTX4*-specific siRNA (**Supplementary Fig. 12a**), then treated the cells with VSV-eGFP, Sendai virus, poly(dA:dT), CpG-A–DOTAP or CpG-A. VSV-eGFP, Sendai virus and poly(dA:dT) induced considerable IRF3 phosphorylation, but CpG-A–DOTAP did not (**Supplementary Fig. 12b**). In contrast, CpG-A–DOTAP, VSV-eGFP and Sendai virus induced considerable IRF7 expression, whereas poly(dA:dT) induced little IRF7 expression (**Supplementary Fig. 12b**). Furthermore, knockdown of endogenous *NLRP4* or *DTX4* expression enhanced IRF3 phosphorylation after viral infection or stimulation with poly(dA:dT). We detected very little IRF7 expression in resting PBMCs, but IRF7 expression was induced much more by infection with VSV-eGFP or Sendai virus in cells transfected with *NLRP4*- or *DTX4*-specific siRNA than in those transfected with scrambled siRNA, whereas treatment with CpG-A–DOTAP induced high IRF7 expression regardless of the status of NLRP4 or DTX4 (**Supplementary Fig. 12b**). These results suggested that NLRP4-DTX4 negatively regulated VSV-eGFP– and Sendai virus–stimulated TBK1-IRF3–dependent type I interferon signaling, which in turn induced IRF7 expression. In contrast, knockdown of *NLRP4* or *DTX4* did not affect IRF7 expression in cells treated with CpG-A–DOTAP. Indeed, *IRF7* mRNA expression was induced at 15 h after infection of PBMCs with VSV-eGFP. Knockdown of *NLRP4* resulted in higher IRF7 expression than that in cells transfected with scrambled siRNA (**Supplementary Fig. 12c**). However, we did not observe such differences in IRF7 expression in cells transfected with *NLRP4*-specific siRNA and treated with CpG-A–DOTAP relative to its expression in cells transfected with scrambled siRNA and treated with CpG-A–DOTAP

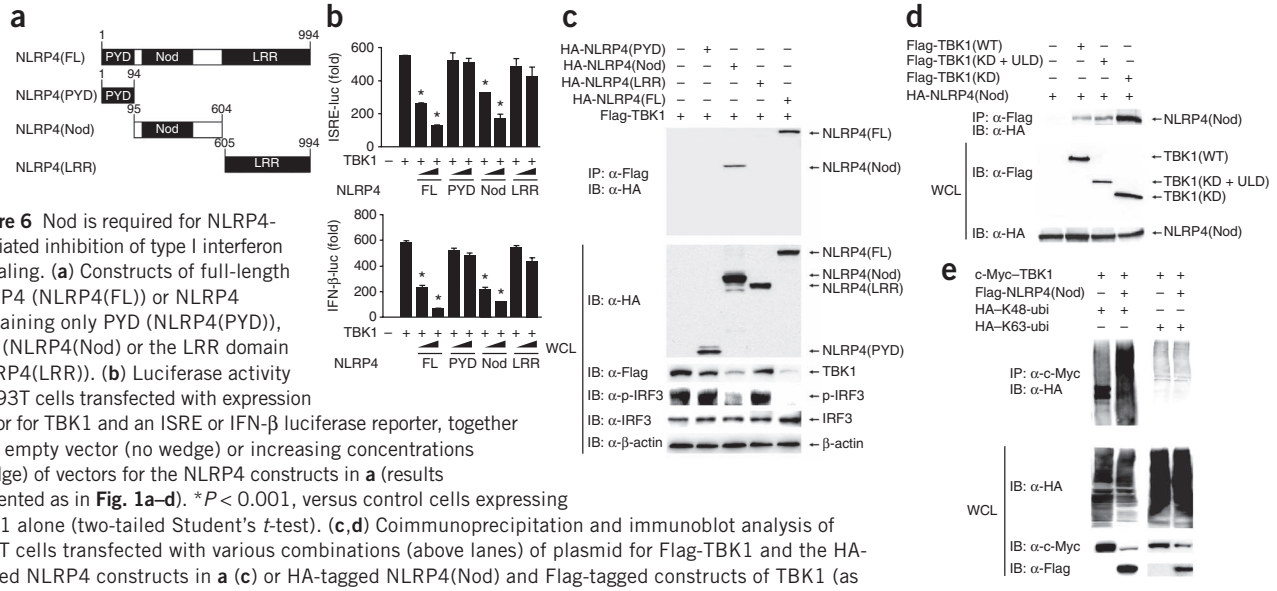

Figure 6 Nod is required for NLRP4-mediated inhibition of type I interferon signaling. (**a**) Constructs of full-length NLRP4 (NLRP4(FL)) or NLRP4 containing only PYD (NLRP4(PYD)), Nod (NLRP4(Nod) or the LRR domain (NLRP4(LRR)). (**b**) Luciferase activity of 293T cells transfected with expression vector for TBK1 and an ISRE or IFN-β luciferase reporter, together with empty vector (no wedge) or increasing concentrations (wedge) of vectors for the NLRP4 constructs in **a** (results presented as in **Fig. 1a–d**). $*P < 0.001$, versus control cells expressing TBK1 alone (two-tailed Student's *t*-test). (**c**,**d**) Coimmunoprecipitation and immunoblot analysis of 293T cells transfected with various combinations (above lanes) of plasmid for Flag-TBK1 and the HA-tagged NLRP4 constructs in **a** (**c**) or HA-tagged NLRP4(Nod) and Flag-tagged constructs of TBK1 (as in **Fig. 3g**; **d**). (**e**) Immunoassay of extracts of 293T cells transfected with plasmid for c-Myc-tagged TBK1, Flag-tagged NLRP4(Nod) and HA-tagged K48-linked or K63-linked ubiquitin, followed by immunoprecipitation with anti-c-Myc beads and immunoblot analysis with anti-HA. Data are representative of three independent experiments (mean and s.d. in **b**).

(**Supplementary Fig. 12c**), which suggested that CpG-A–DOTAP–mediated expression of IRF7 was independent of NLRP4.

We next assessed the secretion of IFN-α, IFN-β, IL-6 and IL-1β after various treatments. Knockdown of *NLRP4* or *DTX4* in PBMCs resulted in much more production of IFN-α and IFN-β after infection with VSV-eGFP or Sendai virus than that in cells transfected with scrambled siRNA (**Supplementary Fig. 12d**,**e**). Treatment with poly(dA:dT) resulted in more production of IFN-β, but not of IFN-α, in cells transfected with *NLRP4*- or *DTX4*-specific siRNA than in cells transfected with scrambled siRNA. In contrast, we observed considerable IFN-α production and little IFN-β production in cells treated with CpG-A–DOTAP but did not observe any difference between cells transfected with *NLRP4*- or *DTX4*-specific siRNA and those transfected with scrambled siRNA in their production of IFN-α and IFN-β (**Supplementary Fig. 12d**,**e**). As expected, CpG-A did not activate type I interferon signaling in PBMCs. We obtained similar results with THP-1 cells transfected with *NLRP4*- or *DTX4*-specific or scrambled siRNA in the presence of various treatments (**Supplementary Fig. 12f**). In addition, we found that Sendai virus induced considerable production of IL-6 and IL-1β in PBMCs, but there was no appreciable difference between cells transfected with *NLRP4* or *DTX4* siRNA and those transfected with scrambled siRNA (**Supplementary Fig. 12d**,**e**).

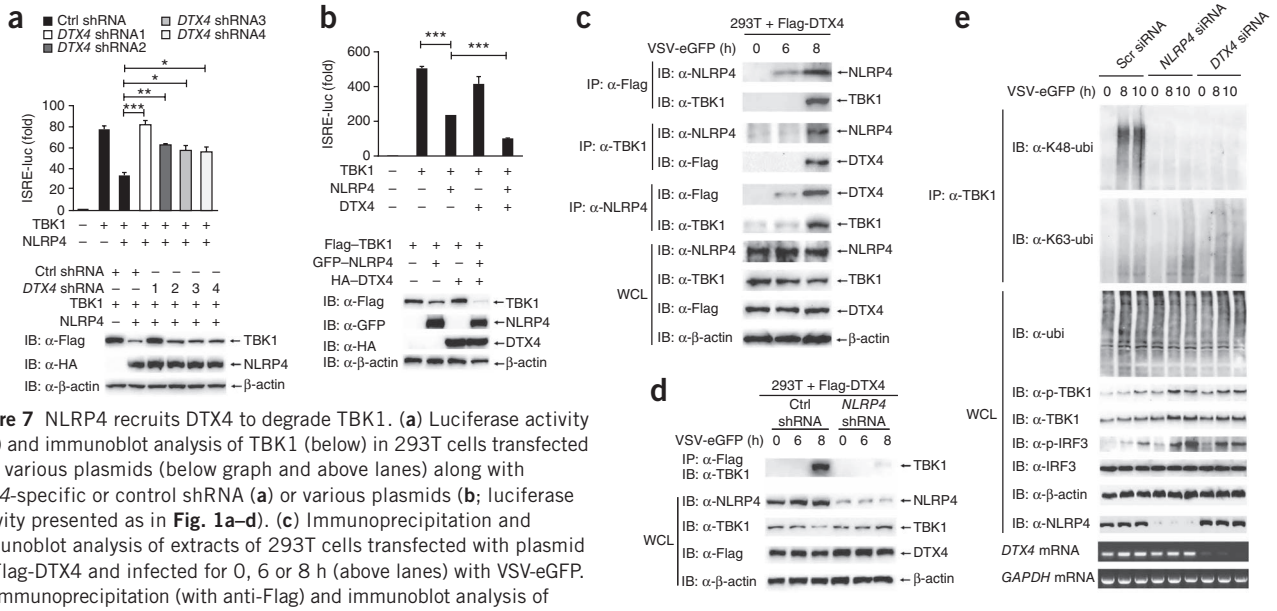

Figure 7 NLRP4 recruits DTX4 to degrade TBK1. (**a**) Luciferase activity (top) and immunoblot analysis of TBK1 (below) in 293T cells transfected with various plasmids (below graph and above lanes) along with *DTX4*-specific or control shRNA (**a**) or various plasmids (**b**; luciferase activity presented as in **Fig. 1a–d**). (**c**) Immunoprecipitation and immunoblot analysis of extracts of 293T cells transfected with plasmid for Flag-DTX4 and infected for 0, 6 or 8 h (above lanes) with VSV-eGFP. (**d**) Immunoprecipitation (with anti-Flag) and immunoblot analysis of extracts of 293T cells transfected with plasmid for Flag-DTX4 and control or *NLRP4*-specific shRNA, then infected for 0, 6 or 8 h (above lanes) with VSV-eGFP. (**e**) Immunoassay of extracts of 293T cells transfected with scrambled, *NLRP4*-specific or *DTX4*-specific siRNA and infected for 0, 8 or 10 h (above lanes) with VSV-eGFP, followed by immunoprecipitation with anti-TBK1 and immunoblot analysis with antibody to K48-linked or K63-linked ubiquitin. Bottom, RT-PCR analysis of *DTX4* mRNA. $*P < 0.05$, $**P < 0.01$ and $***P < 0.001$, versus cells transfected with control shRNA (**a**) or expression vector for TBK1 alone or TBK1 plus NLRP4 (**b**; two-tailed Student's *t*-test). Data are representative of three independent experiments (mean and s.d. in **a**,**b**).

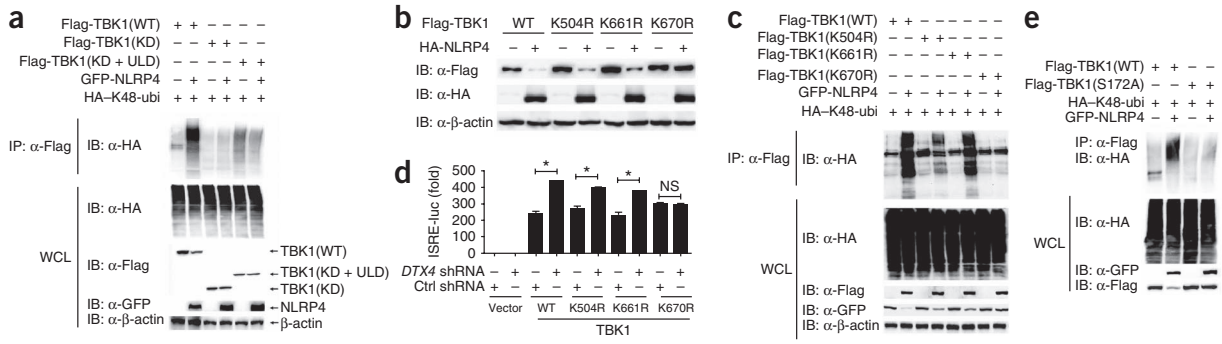

Figure 8 Ubiquitination of TBK1 at Lys670 is essential for NLRP4-DTX4–mediated inhibition of type I interferon signaling. (**a**) Immunoassay of extracts of 293T cells transfected with various combinations (above lanes) of plasmid for GFP-tagged NLRP4 and HA-tagged K48-linked ubiquitin together with Flag-tagged TBK1 constructs (as in **Fig. 3g**), followed by immunoprecipitation with anti-Flag beads and immunoblot analysis with anti-HA. (**b**) Immunoblot analysis of extracts of 293T cells transfected with empty vector or vector for HA-NLRP4, together with plasmid for Flag-tagged wild-type TBK1 or K504R, K661R or K670R mutant of TBK1 (top). (**c**) Immunoprecipitation and immunoblot analysis as in **a** of 293T cells transfected with various combinations (above lanes) of plasmid for GFP-tagged NLRP4 and HA-tagged K48-linked ubiquitin together with plasmid for Flag-tagged TBK1 constructs (as in **b**). (**d**) Luciferase activity of 293T cells transfected with plasmid for Flag-tagged TBK1 constructs (as in **b**) and *DTX4*-specific or control shRNA, together with an ISRE luciferase reporter (presented as in **Fig. 1a–d**). $*P < 0.001$, versus cells transfected with control shRNA (two-tailed Student's *t*-test). (**e**) Immunoprecipitation and immunoblot analysis as in **a** of 293T cells transfected with various combinations (above lanes) of vector for GFP-NLRP4, HA-tagged K48-linked ubiquitin and Flag-tagged wild-type TBK1 or the S172A mutant TBK1. Data are representative of three independent experiments (mean and s.d. in **d**).

These results indicated that NLRP4-DTX4 specifically inhibited TBK1-IRF3–dependent type I interferon signaling but had no effect on MyD88-IRF7–dependent type I interferon signaling.

Lys670 in TBK1 is essential for ubiquitination

Although NLRP4 bound to the kinase domain of activated TBK1, neither TBK1 containing only the kinase domain nor TBK1 containing only the kinase domain and ubiquitin-like domain was ubiquitinated or degraded (**Figs. 3g** and **8a**), which suggested that the coiled-coil domain at the carboxyl terminus of TBK1 may be required for ubiquitination. Using computed-assisted algorithms[17,18], we identified three key ubiquitination sites in the coiled-coil domain of TBK1 and substituted Lys504, Lys661 and Lys670 with arginine (to create K504R, K661R and K670R mutants of TBK1, respectively; **Supplementary Fig. 13a**). We found that the K670R TBK1 mutant almost completely blocked the degradation of TBK1, but the K504R and K661R TBK1 mutants did not (**Fig. 8b**). That finding was further supported by a functional luciferase reporter assay showing that the K670R TBK1 mutant was resistant to the NLRP4-mediated inhibition of activity of the ISRE luciferase reporter (**Supplementary Fig. 13b**). Furthermore, there was no NLRP4-mediated K48-linked ubiquitination of the K670R TBK1 mutant (**Fig. 8c**). Although knockdown of *DTX4* enhanced the activity of the ISRE luciferase reporter in cells transfected to express wild-type TBK1 or the K504R or K661R TBK1 mutant, we did not observe any effect of *DTX4* knockdown on the activity of the ISRE luciferase reporter in cells transfected to express the K670R TBK1 mutant (**Fig. 8d**). Finally, we found that NLRP4 did not induce K48-linked ubiquitination of the S172A TBK1 mutant (**Fig. 8e**), which indicated that phosphorylation of TBK1 was critical for NLRP4-mediated ubiquitination. Together these results suggested that Lys670 in TBK1 was an essential residue for NLRP4-DTX4–mediated K48-linked ubiquitination and degradation of activated TBK1.

On the basis of our findings, we propose the following working model to explain how NLRP4 negatively regulates TBK1 and type I interferon signaling: NLRP4 does not bind to TBK1 or DTX4 in unstimulated or uninfected cells. After infection with virus or stimulation of TLRs, TBK1 is activated by phosphorylation at Ser172 and K63-linked ubiquitination, which triggers IRF3 phosphorylation and type I interferon signaling. Once TBK1 is activated, NLRP4 and DTX4 form a complex through the NLRP4 Nod and the DTX4 RING domain and bind to the kinase domain of the activated form of TBK1; DTX4 functions as an E3 ligase to catalyze K48-linked ubiquitination at Lys670 site in the carboxyl terminus of TBK1 for its proteasomal degradation (**Supplementary Fig. 14**).

DISCUSSION

In this report we have defined a role for NLRP4 in the negative regulation of type I interferon signaling and have shown molecular mechanisms by which NLRP4 targeted activated TBK1 for its degradation through K48-linked ubiquitination of TBK1 by the E3 ubiquitin ligase DTX4. Ectopic expression of NLRP4 inhibited type I interferon signaling activated by ligand stimulation mediated by sensors of RNA and DNA. Conversely, knockdown of *NLRP4* enhanced type I interferon signaling and antiviral immunity. TBK1 is a key component of type I interferon signaling that is activated by various sensors of DNA and RNA, such as RIG-I, Mda5, IFI16 and DDX41, as well as TLR3 and TLR4 (refs. 1,5,6,19–21). Several key adaptors, such as MAVS and STING, as well as TBK1-interacting proteins such as NAP1 and SINTBAD, can activate TBK1, which further phosphorylates and activates IRF3 for type I interferon–responsive gene expression[1,22,23]. A published study has shown that the kinase GSK3β interacts with TBK1 in a viral infection–dependent manner. GSK3β enhances TBK1 self-association and autophosphorylation at Ser172, which is critical for virus-induced IRF3 activation and IFN-β induction[24]. In addition to being activated by phosphorylation, TBK1 can also be activated by ubiquitination at K63 linkages by the ubiquitin ligase NRDP1 after stimulation with lipopolysaccharide or by the E3 ligase MIB1 after infection with an RNA virus[13,14]. It seems that many signaling pathways and adaptors converge at TBK1 activation to trigger IRF3-mediated type I interferon signaling and induce interferon-responsive genes. Because aberrant or uncontrolled innate immune responses may lead to severe or even fatal consequences and chronic inflammatory disease[25,26], TBK1 activation must be tightly controlled. However, how activated TBK1 is inhibited remains poorly understood. Our findings have identified a previously unrecognized role for NLRP4 in the inhibition of type I interferon signaling in which NLRP4 targets TBK1 for its degradation and thus provide molecular insight into the mechanisms of maintaining innate immune homeostasis in response to viral infection.

In elucidating the molecular mechanisms of NLRP4-mediated inhibition of type I interferon signaling, we found that NLRP4 did not interact with TBK1 in unstimulated cells but bound strongly to TBK1 after viral infection, which suggested that the interaction between NLRP4 and TBK1 is signal dependent. That idea was further supported by several lines of evidence. First, the NLRP4 Nod specifically interacted with the kinase domain of TBK1. Second, NLRP4 bound only to the activated (phosphorylated) form of TBK1 but did not bind to the S172A TBK1 mutant, which was unable to activate IRF3. To address how TBK1 is ubiquitinated and degraded, we identified the E3 ligase DTX4 as being involved in this. Notably, the NLRP4 Nod directly interacted with the DTX4 RING domain after viral infection; the NLRP4-DTX4 complex then bound to the activated form of TBK1 for K48-linked polyubiquitination. A published study has shown that PCBP2 interacts with MAVS and ubiquitinates it by recruiting the E3 ligase AIP4, thus leading to degradation of MAVS[27]. In our working model (described above) of the negative regulation of TBK1 and type I interferon signaling by NLRP4, NLRP4 does not bind to TBK1 or DTX4 under normal conditions. However, after viral infection or TLR stimulation, activation of TBK1 triggers IRF3 phosphorylation and type I interferon signaling. Then, NLRP4 and DTX4 form a complex and bind to the activated TBK1, and DTX4 catalyzes K48-linked ubiquitination of TBK1 for its proteasomal degradation.

In determining the role of NLRP4-DTX4 in MyD88-IRF7–dependent (TBK1-independent) type I interferon signaling pathway, we found that NLRP4 did not interact with MyD88 or IRF7 and did not affect MyD88-IRF7–dependent production of IFN-α. Thus, NLRP4-DTX4 specifically inhibited the TBK1-dependent type I interferon signaling pathway in response to viral infection and RNA and DNA stimuli. It has become clear that both NF-κB and type I interferon signaling are tightly regulated through different target molecules and different mechanisms[7,10,28,29]. Although there is only one NLRP4 in humans, seven homologs of NLRP4 (NLRP4a–NLRP4g) have been identified in mice. Two mouse homologs of NLRP4 were able to inhibit type I interferon signaling, which suggested conservation of their role in humans and mice. Because TBK1 has been shown to have a critical role in tumor development mediated by the oncoprotein KRAS and in activating the kinase Akt signaling pathway[19,30–32], we speculate that negative regulation of TBK1 by NLRP4-DTX4 may have an important protective role in cancer development in tissues with high NLRP4 expression. Further studies are needed to investigate the role of NLRP4 in tumor development. Overall, our findings have identified a previously unrecognized role for NLRP4 in the homeostasis of innate immune signaling and have provided molecular insight into the mechanisms by which NLRP4-DTX4 targets activated TBK1 for ubiquitination and degradation.

METHODS

Methods and any associated references are available in the online version of the paper at http://www.nature.com/natureimmunology/.

Note: Supplementary information is available on the Nature Immunology website.

ACKNOWLEDGMENTS

We thank S. Balachandran (Fox Chase Cancer Center) for VSV-eGFP; Y.-J. Liu and Z. Zhang (The University of Texas MD Anderson Cancer Center) for the STING expression plasmid; and A.A. Ajibade for critical reading of the manuscript. Supported by the National Natural Science Foundation of China (31000394 to J.C.), the National Cancer Institute, the US National Institutes of Health (CA090327, CA101795, CA121191, CA116408 and CA094327 to R.-F.W.), the Cancer Research Institute and The Methodist Hospital Research Institute.

AUTHOR CONTRIBUTIONS

J.C., Y.L. and L.Z. designed and did the experiments, J.C. and R.-F.W. wrote the manuscript; D.L. and Z.S. provided reagents and technical assistance; and H.Y.W. and R.-F.W. supervised the project.

COMPETING FINANCIAL INTERESTS

The authors declare no competing financial interests.

Published online at http://www.nature.com/natureimmunology/.
Reprints and permissions information is available online at http://www.nature.com/reprints/index.html.

1. Takeuchi, O. & Akira, S. Pattern recognition receptors and inflammation. *Cell* **140**, 805–820 (2010).
2. Schroder, K. & Tschopp, J. The inflammasomes. *Cell* **140**, 821–832 (2010).
3. Chiu, Y.H., Macmillan, J.B. & Chen, Z.J. RNA polymerase III detects cytosolic DNA and induces type I interferons through the RIG-I pathway. *Cell* **138**, 576–591 (2009).
4. Ablasser, A. *et al.* RIG-I-dependent sensing of poly(dA:dT) through the induction of an RNA polymerase III-transcribed RNA intermediate. *Nat. Immunol.* **10**, 1065–1072 (2009).
5. Zhang, Z. *et al.* The helicase DDX41 senses intracellular DNA mediated by the adaptor STING in dendritic cells. *Nat. Immunol.* **12**, 959–965 (2011).
6. Unterholzner, L. *et al.* IFI16 is an innate immune sensor for intracellular DNA. *Nat. Immunol.* **11**, 997–1004 (2010).
7. Moore, C.B. *et al.* NLRX1 is a regulator of mitochondrial antiviral immunity. *Nature* **451**, 573–577 (2008).
8. Tattoli, I. *et al.* NLRX1 is a mitochondrial NOD-like receptor that amplifies NF-κB and JNK pathways by inducing reactive oxygen species production. *EMBO Rep.* **9**, 293–300 (2008).
9. Benko, S., Magalhaes, J.G., Philpott, D.J. & Girardin, S.E. NLRC5 limits the activation of inflammatory pathways. *J. Immunol.* **185**, 1681–1691 (2010).
10. Cui, J. *et al.* NLRC5 negatively regulates the NF-κB and type I interferon signaling pathways. *Cell* **141**, 483–496 (2010).
11. Jounai, N. *et al.* NLRP4 negatively regulates autophagic processes through an association with beclin1. *J. Immunol.* **186**, 1646–1655 (2011).
12. Fiorentino, L. *et al.* A novel PAAD-containing protein that modulates NF-κB induction by cytokines tumor necrosis factor-alpha and interleukin-1beta. *J. Biol. Chem.* **277**, 35333–35340 (2002).
13. Li, S., Wang, L., Berman, M., Kong, Y.Y. & Dorf, M.E. Mapping a dynamic innate immunity protein interaction network regulating type I interferon production. *Immunity* **35**, 426–440 (2011).
14. Wang, C. *et al.* The E3 ubiquitin ligase Nrdp1 'preferentially' promotes TLR-mediated production of type I interferon. *Nat. Immunol.* **10**, 744–752 (2009).
15. Honda, K. & Taniguchi, T. IRFs: master regulators of signalling by Toll-like receptors and cytosolic pattern-recognition receptors. *Nat. Rev. Immunol.* **6**, 644–658 (2006).
16. Honda, K. *et al.* Spatiotemporal regulation of MyD88-IRF-7 signalling for robust type-I interferon induction. *Nature* **434**, 1035–1040 (2005).
17. Radivojac, P. *et al.* Identification, analysis, and prediction of protein ubiquitination sites. *Proteins* **78**, 365–380 (2010).
18. Xue, Y., Li, A., Wang, L., Feng, H. & Yao, X. PPSP: prediction of PK-specific phosphorylation site with Bayesian decision theory. *BMC Bioinformatics* **7**, 163 (2006).
19. Fitzgerald, K.A. *et al.* IKKepsilon and TBK1 are essential components of the IRF3 signaling pathway. *Nat. Immunol.* **4**, 491–496 (2003).
20. Thurston, T.L., Ryzhakov, G., Bloor, S., von Muhlinen, N. & Randow, F. The TBK1 adaptor and autophagy receptor NDP52 restricts the proliferation of ubiquitin-coated bacteria. *Nat. Immunol.* **10**, 1215–1221 (2009).
21. Weidberg, H. & Elazar, Z. TBK1 mediates crosstalk between the innate immune response and autophagy. *Sci. Signal.* **4**, pe39 (2011).
22. Ryzhakov, G. & Randow, F. SINTBAD, a novel component of innate antiviral immunity, shares a TBK1-binding domain with NAP1 and TANK. *EMBO J.* **26**, 3180–3190 (2007).
23. Chau, T.L. *et al.* Are the IKKs and IKK-related kinases TBK1 and IKK-ε similarly activated? *Trends Biochem. Sci.* **33**, 171–180 (2008).
24. Lei, C.Q. *et al.* Glycogen synthase kinase 3β regulates IRF3 transcription factor-mediated antiviral response via activation of the kinase TBK1. *Immunity* **33**, 878–889 (2010).
25. Liew, F.Y., Xu, D., Brint, E.K. & O'Neill, L.A. Negative regulation of Toll-like receptor-mediated immune responses. *Nat. Rev. Immunol.* **5**, 446–458 (2005).
26. Karin, M., Lawrence, T. & Nizet, V. Innate immunity gone awry: linking microbial infections to chronic inflammation and cancer. *Cell* **124**, 823–835 (2006).
27. You, F. *et al.* PCBP2 mediates degradation of the adaptor MAVS via the HECT ubiquitin ligase AIP4. *Nat. Immunol.* **10**, 1300–1308 (2009).
28. O'Neill, L.A. When signaling pathways collide: positive and negative regulation of toll-like receptor signal transduction. *Immunity* **29**, 12–20 (2008).
29. Xia, X. *et al.* NLRX1 negatively regulates TLR-induced NF-κB signaling by targeting TRAF6 and IKK. *Immunity* **34**, 843–853 (2011).
30. Barbie, D.A. *et al.* Systematic RNA interference reveals that oncogenic KRAS-driven cancers require TBK1. *Nature* **462**, 108–112 (2009).
31. Meylan, E. *et al.* Requirement for NF-κB signalling in a mouse model of lung adenocarcinoma. *Nature* **462**, 104–107 (2009).
32. Ou, Y.H. *et al.* TBK1 directly engages Akt/PKB survival signaling to support oncogenic transformation. *Mol. Cell* **41**, 458–470 (2011).

ONLINE METHODS

Cell culture and reagents. HEK293T, THP-1, RAW264.7 and BxPC-3 cells (American Type Culture Collection) were maintained in DMEM (Mediatech) or RPMI-1640 medium (Invitrogen) containing 10% heat-inactivated FCS. Mouse embryonic fibroblasts were prepared from embryos of C57BL/6 mice at day 15 and were cultured in DMEM supplemented with 10% FBS as described[29]. Buffy coats of blood from healthy donors (from the Gulf Coast Regional Blood Center) were used for isolation of PBMCs by density-gradient centrifugation with Lymphoprep (Nycomed Pharm). The use of PBMCs was in accordance with institutional guidelines and approved protocols by Baylor College of Medicine and The Methodist Hospital Research Institute. Poly (I:C), poly(I:C)-LyoVec and Poly(dA:dT) were from Invivogen.

Antibodies. Anti-NLRP4 (C-20; sc-50623), anti-IRF3 (sc-9082), anti-GFP (FL; sc-8334) and anti-ubiquitin (sc-8017) were from Santa Cruz Biotechnology; horseradish peroxidase–anti-Flag (M2) and anti-β-actin (A1978) were from Sigma; horseradish peroxidase–anti-hemagglutinin (3F10), horseradish peroxidase–anti-c-Myc (11814150001) and unlabeled anti-c-Myc (11667203001) were from Roche Applied Science. Anti-IKKα (IMG-136A) was from Imgenex; antibody to IRF3 phosphorylated at Ser396 (4947), anti-IKKi (2690) and anti-TBK1 (3013) were from Cell Signaling Technology.

Transfection and reporter assays. HEK293T cells (2×10^5) were plated in 24-well plates and transfected, through the use of Lipofectamine 2000 (Invitrogen), with plasmid encoding an NF-κB, IFN-β or ISRE luciferase reporter (firefly luciferase; 100 ng) and pRL-TK (renilla luciferase plasmid; 10 ng) together with 100 ng plasmid encoding Flag-tagged RIG-I, Mda5, MAVS, TBK1 or IKKi, and increasing concentrations (0, 100, or 200 ng) of plasmid encoding HA-NLRP4 or 100 ng plasmid encoding NLRP4 containing the PYD, Nod or LRR domain. Empty pcDNA3.1 vector was used to maintain equal amounts of DNA among wells. Cells were collected at 24 h after transfection and luciferase activity was measured with a Dual-Luciferase Assay (Promega) with a Luminoskan Ascent luminometer (Thermo Scientific) according to the manufacturer's protocol. Reporter gene activity was determined by normalization of the firefly luciferase activity to renilla luciferase activity. An Amaxa nucleofector kit V was used according to the manufacturer's protocols (Lonza Amaxa) for transfection of plasmids or siRNAs into THP-1 cells.

Immunoprecipitation and immunoblot analysis. For immunoprecipitation, whole-cell extracts were prepared after transfection or stimulation with appropriate ligands, followed by incubation overnight with the appropriate antibodies plus Protein A/G beads (Pierce). For immunoprecipitation with anti-Flag or anti-hemagglutinin, anti-Flag or anti-hemagglutinin agarose gels (Sigma) were used. Beads were then washed five times with low-salt lysis buffer, and immunoprecipitates were eluted with 3x SDS Loading Buffer (Cell Signaling Technology) and resolved by SDS-PAGE. Proteins were transferred to nitrocellulose membranes (Bio-Rad) followed by further incubation with the appropriate antibodies. LumiGlo Chemiluminescent Substrate System (KPL) was used for protein detection.

Cytokine-release assay. Human IFN-β was detected with ELISA kits according to the manufacturer's protocols (PBL Biomedical Laboratories).

Cycloheximide-chase assay. Cells were treated for various periods of time with cycloheximide (100 μg/ml) after virus infection, then were collected and analyzed by immunoblot.

Immunofluorescence staining. Cells in culture plates or chamber slides were fixed for 20 min at −20 °C with methanol and nonspecific receptors were blocked with 10% normal goat serum. IRF3 was stained with polyclonal rabbit anti-IRF3 (sc-9082; Santa Cruz Biotechnology), followed by rabbit antibody to Texas red (A-6399; Invitrogen). Nuclei were stained with DAPI (4,6-diamidino-2-phenylindole; Invitrogen). Immunofluorescence staining was visualized and cells were photographed with an Olympus 1X71S1F fluorescence microscope.

Viral infection. VSV-eGFP was provided by S. Balachandran. Cells were infected at various multiplicities of infection as described[10,29].

Statistical analysis. The significance of differences between groups was assessed with a two-tailed Student's *t*-test.

Additional methods. Information on molecular cloning of the gene encoding full-length human NLRP4 and other related genes, real-time PCR analysis and knockdown of *NLRP4* and *DTX4* by RNA-mediated interference is available in the **Supplementary Methods**.

doi:10.1038/ni.2239